Facile Preparation of a Thiol-Reactive ^{18}F-Labeling Agent and Synthesis of ^{18}F-DEG-VS-NT for PET Imaging of a Neurotensin Receptor–Positive Tumor

Zhanhong Wu[1], Lin Li[2], Shuanglong Liu[3], Fumiko Yakushijin[4], Kenichi Yakushijin[4], David Horne[4], Peter S. Conti[3], Zibo Li[3], Fouad Kandeel[1], and John E. Shively[2]

[1]Department of Diabetes and Metabolic Diseases Research, Beckman Research Institute of the City of Hope, Duarte, California; [2]Department of Immunology, Beckman Research Institute of the City of Hope, Duarte, California; [3]Department of Radiology, Molecular Imaging Center, University of Southern California, Los Angeles, California; and [4]Department of Molecular Medicine, Beckman Research Institute of the City of Hope, Duarte, California

Accumulating evidence suggests that neurotensin receptors (NTRs) play key roles in cancer growth and survival. In this study, we developed a simple and efficient method to radiolabel neurotensin peptide with ^{18}F for NTR-targeted imaging. **Methods:** The thiol-reactive reagent ^{18}F-(2-(2-(2-fluoroethoxy)ethoxy)ethylsulfonyl)ethane (^{18}F-DEG-VS) was facilely prepared through 1-step radiofluorination. After high-pressure liquid chromatography purification, ^{18}F-DEG-VS was incubated with the *c*(RGDyC) and *c*(RGDyK) peptide mixture to evaluate its specificity toward the reactive thiol. Thiolated neurotensin peptide was then labeled with ^{18}F using this novel synthon, and the resulting imaging probe was subjected to receptor-binding assay and small-animal PET studies in a murine xenograft model. The imaging results and metabolic stability of ^{18}F-DEG-VS-NT were compared with the thiol-specific maleimide derivative *N*-[2-(4-^{18}F-fluorobenzamido) ethyl]maleimide-neurotensin (^{18}F-FBEM-NT). **Results:** ^{18}F-DEG-VS was obtained in high labeling yield. The reaction of ^{19}F-DEG-VS was highly specific for thiols at neutral pH, whereas the lysine of *c*(RGDyK) reacted at a pH greater than 8.5. ^{18}F-DEG-VS-*c*(RGDyC) was the preferred product when both *c*(RGDyK) and *c*(RGDyC) were incubated together with ^{18}F-DEG-VS. Thiolated neurotensin peptide (Cys-NT) efficiently reacted with ^{18}F-DEG-VS, with a 95% labeling yield (decay-corrected). The radiochemical purity of the ^{18}F-DEG-VS-NT was greater than 98%, and the specific activity was about 19.2 ± 4.3 TBq/mmol. Noninvasive small-animal PET demonstrated that ^{18}F-DEG-VS-NT had an NTR-specific tumor uptake in subcutaneous HT-29 xenografts. The tumor-to-muscle, tumor-to-liver, and tumor-to-kidney ratios reached 30.65 ± 22.31, 11.86 ± 1.98, and 1.91 ± 0.43 at 2 h after injection, respectively, based on the biodistribution study. Receptor specificity was demonstrated by blocking experiment. Compared with ^{18}F-FBEM-NT, ^{18}F-DEG-VS-NT was synthesized with fewer steps and provided significantly improved imaging quality in vivo. **Conclusion:** We have established a facile ^{18}F-labeling method for site-specific labeling of the Cys-NT. Using this method, we synthesized an NTR-targeted PET agent, which demonstrated high tumor-to-background contrast.

Received Jan. 15, 2014; revision accepted Mar. 17, 2014.

For correspondence contact either of the following:
Zibo Li, USC Molecular Imaging Center, 2250 Alcazar St. CSC 103, Los Angeles, CA 90033.
E-mail: ziboli@usc.edu
John E. Shively, Department of Immunology, Beckman Research Institute of the City of Hope, 1500 East Duarte Rd., Duarte, CA 91010.
E-mail: JShively@coh.org

Published online May 22, 2014.

Key Words: ^{18}F; vinyl sulfone; neurotensin; PET

J Nucl Med 2014; 55:1178–1184
DOI: 10.2967/jnumed.114.137489

PET imaging with ^{18}F has several attributes that make it clinically attractive, including nearly 100% positron efficiency, very high specific radioactivity, and a short half-life of ^{18}F (109.8 min) (*1*). Moreover, its low positron energy and attendant short positron linear range in tissue result in higher resolution in PET imaging than other more energetic positron emitters. On the other hand, the half-life of ^{18}F is sufficient to allow syntheses, transportation, and imaging procedures to be extended over several hours, while the patient is subjected to a limited amount of radiation exposure. Recently, ^{18}F-labeled biomolecules, including peptides with short biologic half-lives, are gaining increasing importance for PET imaging studies of receptor expression and activity in living subjects. However, direct labeling of peptides with ^{18}F typically results in poor incorporation yields, and the harsh conditions (such as high temperature, high pH, anhydrous conditions, and organic solvents) may lead to degradation of the peptide ligands. Therefore, peptides are typically labeled with ^{18}F by an indirect strategy that involves incorporating ^{18}F into a prosthetic group first, followed by conjugation to the peptide precursor under mild conditions (*2–8*).

Because free thiol groups are not as common as amino and carboxylic acid in most peptides and proteins, thiol-reactive prosthetic groups have been used to modify peptides and proteins at specific sites, providing an ^{18}F-labeling approach with high chemoselectivity in contrast to the carboxylate and amine-reactive reagents (*9–12*).

Despite some encouraging results, most thiol-reactive synthons require multistep reactions that are time-consuming and labor-intensive. Thus, there is a clear need to develop a more facile procedure for ^{18}F labeling of thiols. Vinyl sulfone (VS) holds several advantages for ^{18}F labeling of thiol groups, compared with ^{18}F-labeled maleimide. First, the product from the reaction of thiol with VS yields a single stereoisomer structure, unlike maleimide conjugates, which have 2 potential stereoisomers (*13,14*). Second, ^{18}F-VS synthon might be obtained through a 1-step ^{18}F-fluorination, greatly simplifying the synthetic procedure. And third, VS

conjugates are stable in aqueous solution for extended periods and are not subject to hydrolysis at neutral pH like maleimide conjugates (*15–19*). Thus, VS has an excellent potential for conjugation to thiol-containing peptides or other biomolecules even when used in aqueous buffer conditions.

In this study, we report the development of a novel ^{18}F-labeling agent, ^{18}F-(2-(2-(2-fluoroethoxy)ethoxy)ethylsulfonyl)ethane (^{18}F-DEG-VS), for conjugation to free thiol groups in bioligands. Because accumulating evidence suggests that neurotensin receptors (NTRs) play key roles in cancer growth and survival (*20,21*), a thiolated neurotensin (NT) peptide was used to test the potential of ^{18}F-DEG-VS as a peptide-labeling agent. The resulting ^{18}F-labeled-NT derivative was further evaluated by PET in a rodent model with an NTR1-positive tumor.

MATERIALS AND METHODS

General

All commercially available chemical reagents were purchased from Aldrich and used without further purification. *c*(RGDyC) and *c*(RGDyK) were purchased from Peptides International Inc. A thiolated NT peptide analog was synthesized by the City of Hope peptide synthesis core using standard FMOC chemistry. No-carrier-added ^{18}F-fluoride was produced via the ^{18}O(p, n)^{18}F reaction. All high-performance liquid chromatography (HPLC) conditions are gradient. HPLC methods, nuclear magnetic resonance spectra, and mass spectrometry details are listed in the supplemental material (available at http://jnm.snmjournals.org).

Chemistry

Detailed synthetic procedures and characterizations were provided as supplemental material for 2-(2-hydroxyethoxy)ethyl 4-nitrobenzenesulfonate (**1**), 2-(2-(2-(vinylsulfonyl)ethoxy)ethoxy)ethyl 4-nitrobenzenesulfonate (**2**), (2-(2-(2-fluoroethoxy)ethoxy)ethylsulfonyl)ethene (^{19}F-DEG-VS, **3**), ^{19}F-DEG-VS-c(RGDyC), ^{19}F-DEG-VS-c(RGDyK), ^{19}F-DEG-VS-NT, ^{19}F-DEG-VS-(Ac)-NT, ^{19}F-FBEM-c(RGDyC), and ^{19}F-FBEM-NT.

Radiochemistry

Detailed labeling procedures and characterizations were provided as supplemental material for ^{18}F-DEG-VS, ^{18}F-DEG-VS-c(RGDyC), ^{18}F-DEG-VS-c(RGDyK), ^{18}F-DEG-VS-NT, ^{18}F-DEG-VS-(Ac)-NT, ^{18}F-FBEM-c(RGDyC), and *N*-[2-(4-^{18}F-fluorobenzamido)ethyl]maleimide-neurotensin (^{18}F-FBEM-NT).

Selectivity Test: c(RGDyK) and c(RGDyC). ^{18}F-DEG-VS (100 μL, 37 MBq [1 mCi]) and 50 μL of borate buffer (pH 8.5) were added into *c*(RGDyC) (100 μg, 0.16 μmol) and *c*(RGDyK) (105 μg, 0.16 μmol). The reaction mixture was incubated at room temperature for 30 min. The reaction was quenched by acetic acid (5%, 600 μL), and the product was analyzed by radio-HPLC using Method 1 (supplemental data).

Cells and Animals

The human colon adenocarcinoma cell HT-29 was obtained from American Type Culture Collection. Animal procedures were performed according to a protocol approved by the University of Southern California Institutional Animal Care and Use Committee. In the procedure, 4- to 6-wk-old male athymic mice (BALB/c *nu/nu*; weight, 20–30 g) were injected subcutaneously with HT-29 human colon adenocarcinoma cells at a concentration of 1×10^6 cells per 0.1 mL in the shoulder, and enough time was allowed for tumors to grow to at least 3 mm in diameter.

In Vitro Cell-Binding Assay

The in vitro NTR1-binding affinities of ^{19}F-DEG-VS-NT and NT(8-13) were assessed via competitive cell-binding assays using ^{125}I-NT (8-13) (PerkinElmer) as described previously (supplemental material) (*22*).

Biodistribution and Small-Animal PET Imaging of HT-29 Tumor Xenografts in Mice

Small-animal PET imaging was performed in nude mice bearing HT-29 colorectal xenografts after tail vein injection with 3.7 MBq of ^{18}F-DEG-VS-NT or ^{18}F-FBEM-NT ($n = 3$, respectively). For blocking studies, NT(8-13) (100 μg) was coinjected with ^{18}F-DEG-VS-NT ($n = 3$). Serial imaging (0.5, 1, and 2 h after injection; scan duration, 5, 5, and 10 min, respectively) was performed using a small-animal PET R4 scanner (Siemens Medical Solutions, Inc.).

Biodistributions were performed in nude mice bearing HT-29 colorectal xenografts. Animals were sacrificed under inhalation anesthesia at 2 h after injection of 3.7 MBq of ^{18}F-DEG-VS-NT. Tissues and organs of interest were excised and weighed. Radioactivity in each excised specimen was measured using a γ counter; radioactivity uptake was expressed as percentage injected dose per gram (%ID/g). The mean uptake (%ID/g) and corresponding SD was calculated for each group of animals.

In Vivo Metabolic Stability

The in vivo metabolic stability of ^{18}F-DEG-VS-NT and ^{18}F-FBEM-NT was evaluated in nude mice bearing HT-29 tumors (supplemental material). For ^{18}F-DEG-VS-*c*(RGDyC) and ^{18}F-FBEM-*c*(RGDyC), the urine samples were collected and analyzed by HPLC.

Statistical Analysis

Quantitative data were expressed as mean ± SD. Means were compared using 1-way ANOVA and the Student *t* test. *P* values of less than 0.05 were considered statistically significant.

RESULTS

Chemistry

As shown in Figure 1, the F-DEG-VS precursor [2-(2-(2-(vinylsulfonyl)ethoxy)ethoxy) ethyl 4-nitrobenzenesulfonate **2** was synthesized in 20% yield after a 2-step reaction and was ^{19}F-fluorinated by reacting with tetrabutylammonium fluoride (TBAF). ^{19}F-DEG-VS was used as a chemical standard for ^{18}F-DEG-VS and the starting material for the following reactions.

We first evaluated the cold reaction between ^{19}F-DEG-VS and *c*(RGDyC) (with a free SH group) and *c*(RGDyK) (with a free NH_2 group) peptides (Fig. 2A). Both *c*(RGDyC) and *c*(RGDyK) reacted with ^{19}F-DEG-VS; however, *c*(RGDyK) reacted only at a pH higher than 8.5 after overnight incubation, compared with a pH of 7.0 and 30-min incubation for *c*(RGDyC) (Fig. 2B).

Thiolated NT also reacted with ^{19}F-DEG-VS efficiently. However, 2 products (^{19}F-DEG-VS-NT and (^{19}F-DEG-VS)$_2$-NT) (Figs. 3A and 3B) were obtained when the reaction was performed at a high pH (e.g., pH 8.5), due to the reaction of F-DEG-VS with 1 thiol and 1 amine group present in our NT analog.

Radiochemistry

The ^{18}F labeling of the VS synthon was tested at various solvent, concentration, and temperature conditions. With 10-mg precursor loading, the representative radio-HPLC trace of the crude labeling reaction is shown in Figure 1B. Although the radiolabeling yield for ^{18}F-DEG-VS was calculated to be 90% yield based on HPLC integration, the isolation yield was 35% ± 6%. The discrepancy between these 2 calculation methods could be caused by the activity that was bound to reaction vessel walls and the head of HPLC columns. ^{18}F-DEG-VS demonstrated good stability, and the radiochemical purity was still more than 99% at 4 h after HPLC purification after incubation in phosphate-buffered saline (Fig. 2C).

For the radiolabeling reaction, we incubated equal molar amounts of *c*(RGDyC) and *c*(RGDyK) with ^{18}F-DEG-VS in

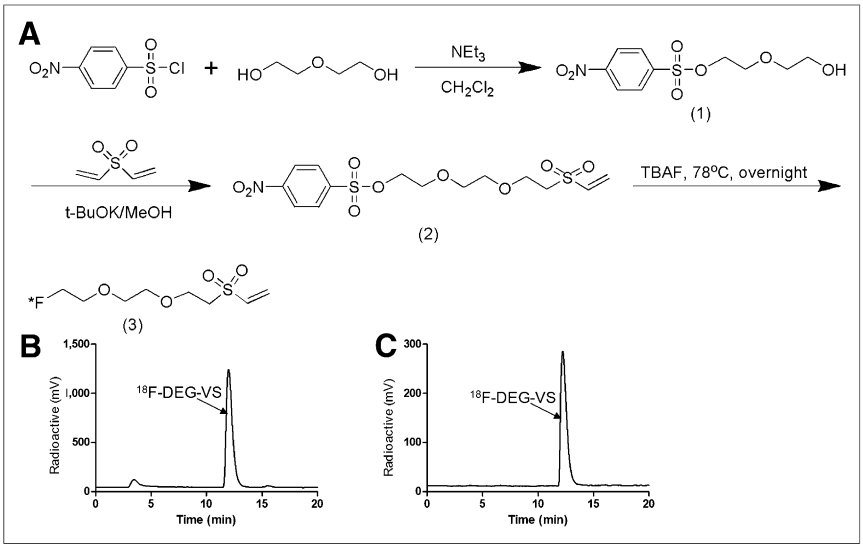

FIGURE 1. (A) Synthetic scheme of F-DEG-VS. (B) HPLC profile of crude reaction of ^{18}F-DEG-VS. (C) HPLC profile of ^{18}F-DEG-VS at 4 h after purification.

the same reactor. In this case, we observed only the product from *c*(RGDyC) and ^{18}F-DEG-VS (Fig. 2B). The absence of product from *c*(RGDyK)/^{18}F-DEG-VS demonstrated the selectivity of this reaction for the thiol over the amino group. Thus, even at pH 8.5, ^{18}F-DEG-VS selectively labeled the thiol group in the presence of a free amino group.

^{18}F-DEG-VS also efficiently reacted with thiolated NT. The (F-DEG-VS)$_2$-NT byproduct seen with the ^{19}F synthesis was not observed in radiolabeling reactions as shown by HLPC (Fig. 3C). The radiochemical purity of ^{18}F-DEG-VS-NT was still greater than 95% at 5 h after HPLC purification after incubation in phosphate-buffered saline (Supplemental Fig. 1). To compare ^{18}F-DEG-VS with a thiol-specific maleimide-based reagent, ^{18}F-FBEM was also prepared and shown to react efficiently with *c*(RGDyC) and thiolated NT, respectively (Supplemental Fig. 2).

In Vitro Cell-Binding Affinity

We compared the receptor-binding affinity of ^{19}F-DEG-VS-NT with that of NT(8-13) using a competitive cell-binding assay (Fig. 4). Both peptides inhibited the binding of ^{125}I-NT(8-13) to NTR1-positive HT-29 cells in a dose-dependent manner. The IC_{50} (the half maximal inhibitory concentration) value for ^{19}F-DEG-VS-NT (2.03 ± 0.22 nmol/L) was comparable to that of NT(8-13) (2.12 ± 0.26 nmol/L). The results clearly demonstrated that F-DEG-VS-NT has an in vitro receptor-binding affinity to NTR1 similar to NT(8-13).

Biodistribution and Small-Animal PET Imaging

The NTR1-targeting efficacy of ^{18}F-DEG-VS-NT was evaluated in HT-29 xenografts (NTR1-positive) at multiple time points (0.5, 1, and 2 h after injection) with small-animal PET. As shown in Figure 5A, the HT-29 tumors were clearly visualized with high tumor-to-background contrast for ^{18}F-DEG-VS-NT, and the tumor uptake was 1.30 ± 0.17, 0.96 ± 0.29, and 0.63 ± 0.20 %ID/g at 0.5, 1, and 2 h after injection, respectively. In comparison, ^{18}F-FBEM-NT also demonstrated prominent uptake in tumors (0.13 ± 0.08 %ID/g, 2 h after injection) but was significantly (P = 0.017) lower than observed for ^{18}F-DEG-VS-NT (2 h after injection). The liver and kidney uptake of ^{18}F-FBEM-NT was 0.28 ± 0.03 and 0.64 ± 0.02 %ID/g at 2 h after injection, respectively. Compared with ^{18}F-FBEM-NT, ^{18}F-DEG-VS-NT exhibited superior tumor-to-background contrast and lower abdomen background (Supplemental Fig. 3).

The NTR1 specificity of ^{18}F-DEG-VS-NT was confirmed by a blocking experiment in which the radiotracer was coinjected with an excess of unlabeled NT(8-13). As can be seen from Figure 5A, in the presence of unlabeled NT(8-13), the NTR1 tumor uptake (0.47, 0.15, and 0.04 %ID/g at 0.5, 1, and 2 h after injection, respectively) was significantly ($P < 0.01$) lower than that without NT(8-13) blocking at all time points. The kidney uptake rapidly decreased from 6.82 ± 2.90 %ID/g at 0.5 h after injection to 0.17 ± 0.01 %ID/g at 2 h after injection. On the basis of imaging analysis, tumor-to-kidney, tumor-to-liver, and tumor-to-muscle ratios were 3.69 ± 1.50, 10.33 ± 4.01, and 27.12 ± 5.46 at 2 h after injection, respectively. At 2 h after injection, significantly higher uptake was demonstrated in the tumors than in the kidney, liver, and muscle. Other organs, including heart and lung, were essentially at background levels by 2 h after injection.

In addition to the small-animal PET study, we also performed biodistribution studies using a separate group of HT-29 tumor–bearing mice at 2 h after injection of ^{18}F-DEG-VS-NT. As shown in Figure 5B, the tumor and kidney uptake was 0.86 ± 0.09 and 0.46 ± 0.05 %ID/g, respectively. At 2 h after injection, significantly higher uptake was demonstrated in the tumors than in the kidney, liver, and muscle (Fig. 5B). Other organs, including the heart and lung, were essentially at background levels by 2 h after injection.

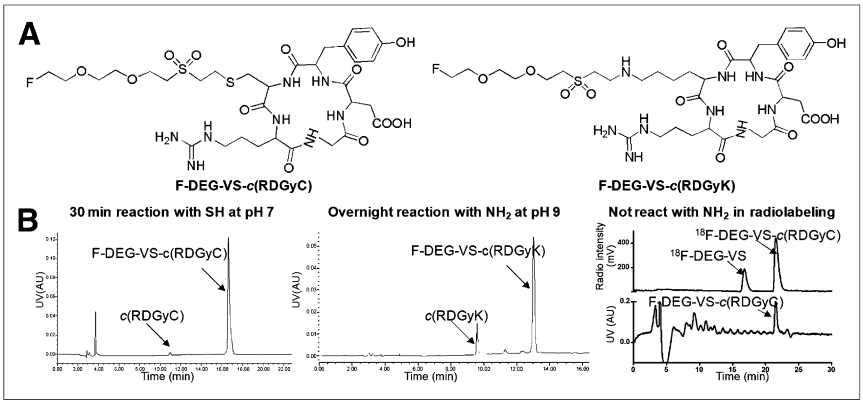

FIGURE 2. (A) Chemical structure of F-DEG-VS-*c*(RGDyC) and F-DEG-VS-*c*(RGDyK). (B) HPLC profile of crude reaction of ^{19}F-DEG-VS-*c*(RGDyC), ^{19}F-DEG-VS-*c*(RGDyK), ^{18}F-DEG-VS with *c*(RGDyC)/*c*(RGDyK) (radio), and standard of ^{19}F-DEG-VS-*c*(RGDyC) on radio-HPLC (UV). AU = arbitrary units; UV = ultraviolet.

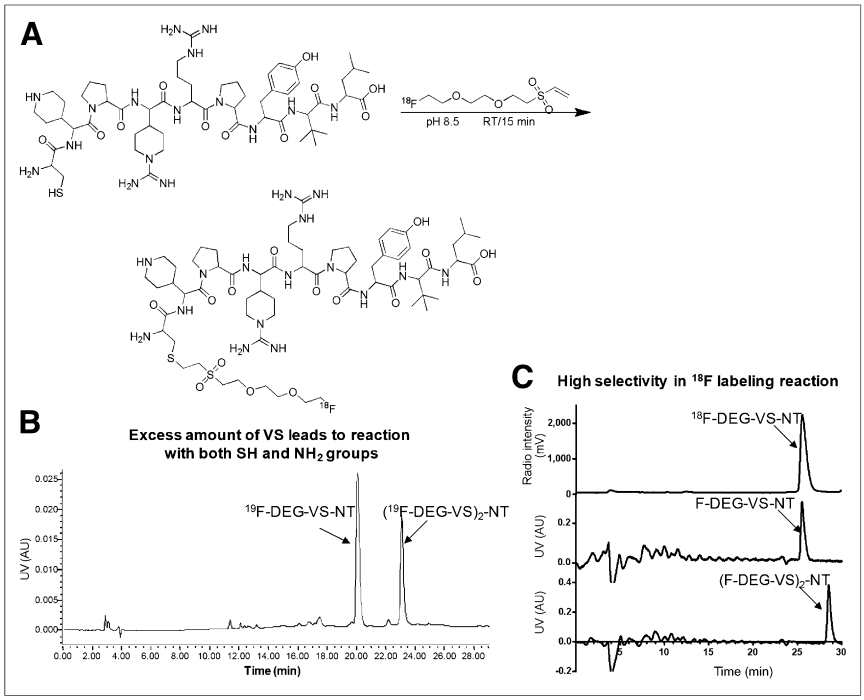

FIGURE 3. (A) Radiosynthesis scheme of ^{18}F-DEG-VS-NT. (B) HPLC profile of crude reaction of ^{19}F-DEG-VS and NT. (C) HPLC profiles of ^{18}F-DEG-VS-NT (radioactive) ^{19}F-DEG-VS-NT (UV), and (^{19}F-DEG-VS)$_2$-NT (UV). AU = arbitrary units; UV = ultraviolet.

Metabolic Stability Study

The metabolic stability of ^{18}F-DEG-VS-NT was determined in mouse urine and in the liver, kidneys, and HT-29 tumor homogenates at 1 h after injection. The high-performance liquid chromatograms are shown in Supplemental Figure 4. The retention time of intact ^{18}F-DEG-VS-NT was 18.50 min. A major metabolite peak was found at about 20 min for the tumor, and 2 major metabolite peaks were found at 13–15 and 17 min for urine, kidney, and liver samples. No significant defluorination was observed throughout the study. The metabolic stability of ^{18}F-FBEM-NT was also studied.

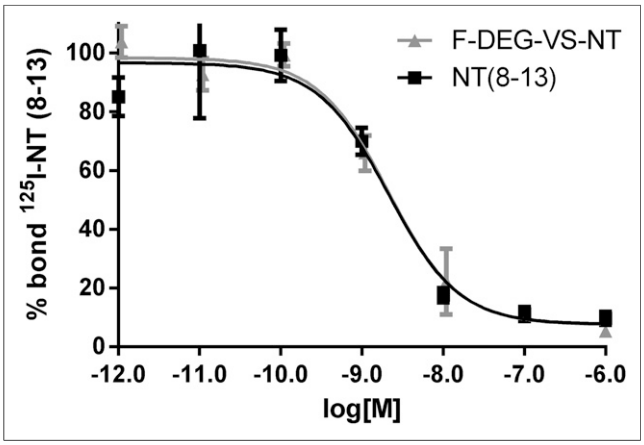

FIGURE 4. Competitive binding assays of ^{125}I-NT(8-13) and ^{19}F-DEG-VS-NT or NT(8-13) in HT-29 cells. Data are mean ± SD (n = 3). x-axis reflects concentration of nonradiolabeled competitor. IC_{50} values for ^{19}F-DEG-VS-NT and NT(8-13) were 2.03 ± 0.22 and 2.12 ± 0.26 nmol/L, respectively.

The retention time of intact ^{18}F-FBEM-NT was 19.02 min. Besides the multiple peaks between 15 and 21 min, there was a major peak at about 5 min for tumor, kidney, and liver. There was no substantial peak for unmetabolized material in the tumor at 1 h after injection. We also synthesized the ^{18}F-DEG-VS-c(RGDyC) and ^{18}F-FBEM-c(RGDyC) and analyzed their urine metabolites. Unlike the unstable NT peptide, the c(RGDyC) is stable in vivo. Accordingly, ^{18}F-DEG-VS-c(RGDyC) gave a single peak corresponding to intact labeled peptide excreted in urine (Supplemental Fig. 5). ^{18}F-FBEM-c(RGDyC) also gave a major peak, with evidence of small amounts of other components (Supplemental Fig. 6).

DISCUSSION

Accumulating evidence suggests that NTRs play key roles in cancer growth and survival (*20,23,24*). In fact, NTRs have been proposed as a promising marker for human pancreatic carcinoma (*25*), breast cancer (*26*), head and neck carcinoma (*27*), prostate cancer (*28*), and non–small cell lung cancer (*29*).

The development of imaging agents to obtain NTR expression profiles or fingerprints of individual tumors could therefore lead to efficient early-stage diagnosis and customized treatment options for cancer patients. NT, a tridecapeptide ligand for NTR, is metabolized rapidly in plasma by endogenous peptidases. To improve the in vivo stability, various NT analogs have been developed. For example, several radiolabeled NT analogs were recently developed as a valuable tool for both imaging and therapy of NTR-positive tumors (*30–35*). Although encouraging results have been obtained in these initial studies, the relatively high kidney uptake and suboptimal tumor-to-tissue contrast warrant further improvement of these agents, especially in the choice of the radiolabel. Previously, we have demonstrated that the pharmacokinetics of peptide-based PET probes improved significantly by substituting ^{18}F in place of ^{64}Cu (*36,37*). In fact, as one of the commonly used PET radioisotopes, ^{18}F can also be easily produced in high quantities in a medical cyclotron, with an ideal half-life of 110 min for imaging applications. Therefore, we have devoted a significant amount of effort to develop a ^{18}F-labeled PET probe for NTR-targeted imaging.

Because cysteines are much less abundant than lysines, aspartic acid, and glutamic acid residues in peptides and proteins, thiol-reactive agents have been used to site-selectively modify these biomolecules. Previously, several thiol-reactive ^{18}F synthons have been reported, most of which bear a maleimide group for conjugate addition of thiols under mild conditions. However, maleimide-based synthons require multistep reactions, which are time-consuming and labor-intensive. In recognition of these issues, we set out to develop a platform technology based on the Michael addition reactivity of vinyl sulfone. VS chemistry has been demonstrated to be suitable

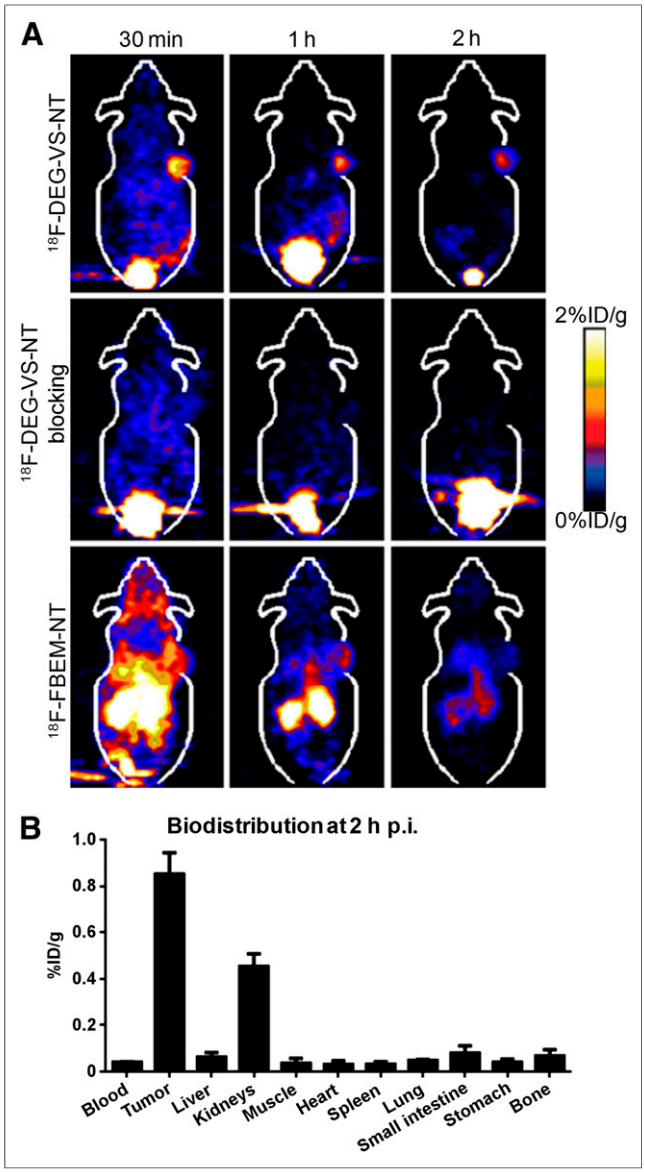

FIGURE 5. (A) Representative coronal small-animal PET images of mice bearing HT-29 xenografts after injection of 3.7 MBq of ^{18}F-DEG-VS-NT without (upper) and with unradiolabeled NT(8-13) (middle) and 3.7 MBq of ^{18}F-FBEM-NT (lower). (B) Biodistribution of ^{18}F-DEG-VS-NT in mice bearing HT-29 xenograft at 2 h after injection (p.i.).

for the selective modification of cysteine residues under mild conditions (*15*). The water stability of the VS function, the lack of byproducts, the almost quantitative yields of the reaction with thiols, and the chemical stability of the thioether linkage formed make this reaction an appealing approach for ^{18}F labeling.

Our VS-based prosthetic group was designed to be hydrophilic, a highly desirable attribute for in vivo applications. To simplify the labeling procedures, initial efforts were focused on a 1-step radiofluorination of VS. Radiofluorination reactions were performed in MeCN/dimethyl sulfoxide using azeotropically dried ^{18}F-TBAF. Conversion of VS synthon to the corresponding ^{18}F-DEG-VS was found to be strongly dependent on the VS synthon reaction concentration and temperature. Under optimized conditions, greater than 90% labeling yield could be obtained within 15 min based on HPLC integration. The isolated yield was determined to be 35% ± 6%.

Because VS may also react with primary amines at high pH (*15*), we decided to explore the selectivity of the VS synthon reaction under neutral pH conditions. Although both *c*(RGDyK) and *c*(RGDyC) efficiently react with ^{19}F-DEG-VS reagent, *c*(RGDyK) is much less reactive, which required overnight incubation and higher pH, compared with 30-min incubation for *c*(RGDyC). Moreover, with the ^{18}F-DEG-VS reagent, only *c*(RGDyC) reacted in the equimolar mixture of *c*(RGDyK) and *c*(RGDyC). This result clearly demonstrated the chemoselectivity of ^{18}F-DEG-VS toward the SH functional group.

After establishing an efficient ^{18}F-DEG-VS–labeling method, thiolated NT peptide was labeled with ^{18}F. ^{18}F-DEG-VS-NT was obtained in greater than 95% yield within 35 min, and the radiochemical purity was more than 99%. The specific radioactivity of ^{18}F-DEG-VS-NT was determined on the basis of a literature method (*38*) in which the ultraviolet integration of final product was compared with a standard titration curve, yielding a specific radioactivity of 19.2 ± 4.3 TBq/mmol for ^{18}F-DEG-VS-NT.

Because the chemical modification of a peptide can significantly decrease receptor binding affinity, an in vitro cell-binding assay of ^{19}F-DEG-VS-NT and NT(8-13) was performed. The difference of the binding affinity between ^{19}F-DEG-VS-NT and NT (8-13) was negligible, as supported by the similar IC_{50} values. The imaging quality of ^{18}F-DEG-VS-NT was evaluated in vivo using an HT-29 xenograft model, which has been well established to have high NTR1 expression (*20*). ^{18}F-DEG-VS-NT had a rapid renal clearance. ^{18}F-DEG-VS-NT predominantly accumulated in the kidneys (6.82 ± 2.90 %ID/g) at 30 min after injection and quickly decreased to 1.19 ± 0.49 %ID/g at 1 h after injection and 0.17 ± 0.01 %ID/g at 2 h after injection. In the blocking experiment, nonradioactive NT peptide significantly ($P < 0.01$) inhibited the tumor uptake of ^{18}F-DEG-VS-NT (Fig. 5A) at all time points, clearly demonstrating the receptor specificity of this imaging agent. Because the tracer has low uptake in the abdominal region, we also performed a biodistribution study to determine the uptake in liver, kidney, small intestine, spleen, stomach, and other organs or tissues more accurately. As shown in Figure 5B, the uptake in these organs was close to background level, correlating well with the high-contrast tumor image obtained from the small-animal PET scan. Because the activity decreased rapidly in all major organs, a high tumor-to-organ ratio was obtained at 2 h after injection, including tumor to muscle (30.65 ± 22.31), tumor to liver (11.86 ± 1.98), and tumor to kidneys (1.91 ± 0.43), calculated by biodistribution study. Because NT peptide has 2 potential reactive sites, (Ac)-NT was additionally synthesized, which could also be efficiently labeled with ^{18}F-DEG-VS (Supplemental Fig. 7). It still needs to be determined whether this new agent will have tumor-targeting capability similar to ^{18}F-DEG-VS-NT.

Although the major focus of this report was the development of a new thiol-specific, ^{18}F-radiolabeling method for peptides and its evaluation by PET imaging, it was also important to perform a direct in vivo comparison with an existing maleimide-based reagent to demonstrate the potential advantages and limitations of our newly developed labeling strategy. Therefore, a maleimide-based reagent, namely ^{18}F-FBEM-NT, was also synthesized for a direct comparison of imaging quality and metabolic stability. As shown

in Supplemental Figure 2, ^{18}F-FBEM-NT was a more complicated synthesis involving 5 steps: fluorination, hydrolysis, activation of the carboxyl group, reaction with the maleimide derivative, and conjugation with Cys-NT. In comparison, the synthesis of ^{18}F-DEG-VS-NT involves only 2 steps: fluorination of the synthon and conjugation to Cys-NT. Importantly on PET imaging, ^{18}F-FBEM-NT demonstrated significantly higher background and lower contrast than ^{18}F-DEG-VS-NT (Supplemental Fig. 3). To determine whether the lower abdominal background and high tumor uptake observed for ^{18}F-DEG-VS-NT, compared with ^{18}F-FBEM-NT, were caused by a difference in metabolism, a metabolic stability study was performed. As shown in Supplemental Figure 4, both ^{18}F-DEG-VS-NT and ^{18}F-FBEM-NT exhibited several metabolites in vivo. However, a major metabolite peak at about 5 min was found for ^{18}F-FBEM-NT but not for ^{18}F-DEG-VS-NT. Nonetheless, because of the short half-life of NT in humans and rodents (*39,40*), a conclusion cannot be drawn based on just the above experiments. In a further approach, we have conjugated the more metabolically stable *c*(RGDyC) peptide with both synthons and studied the urine metabolism of ^{18}F-FBEM-*c*(RGDyC) and ^{18}F-DEG-VS-*c*(RGDyC). As shown in Supplemental Figures 5 and 6, ^{18}F-FBEM-*c*(RGDyC) has additional metabolites in urine not seen for ^{18}F-DEG-VS-*c*(RGDyC). This experiment suggests that our VS-based synthon is more stable in vivo than the maleimide-based synthon. Thus, the metabolites observed in the ^{18}F-DEG-VS-NT study may be caused mainly by the degradation of the NT peptide and not the synthon itself. Clearly, the stability benefit of the DEG-VS linker, compared with the maleimide linker, may also depend on the peptide to which it is conjugated. Although maleimide-based synthons such as ^{18}F-FBEM are expected to be unstable based on literature reports, they may still perform well within the time scale of an ^{18}F imaging study. The observed superior contrast of ^{18}F-DEG-VS-NT, compared with ^{18}F-FBEM-NT, in an animal model warrants consideration of clinical translation of this agent for NTR-targeted imaging in humans.

CONCLUSION

We have established a novel ^{18}F-labeling method for site-specific labeling a free thiol group present or introduced into peptide or proteins. Using this novel method, we synthesized a NTR1-targeted PET imaging agent, which demonstrated specific tumor uptake and superior tumor-to-background contrast. The elevated tumor–to–major-organ uptake ratios (including tumor to kidney) led to high-contrast images at 2 h after injection. The low background in normal tissues should allow the detection of small tumors (especially at the abdomen area) by PET imaging ^{18}F-DEG-VS-NT.

DISCLOSURE

The costs of publication of this article were defrayed in part by the payment of page charges. Therefore, and solely to indicate this fact, this article is hereby marked "advertisement" in accordance with 18 USC section 1734. This work was supported by a grant from Larry L. Hillblom Foundation (2013-D-015-SUP), the Jonas Bros Foundation, the Juvenile Diabetes Research Foundation (37-2011-638), the American Cancer Society (121991-MRSG-12-034-01-CCE), and the USC Department of Radiology. No other potential conflict of interest relevant to this article was reported.

REFERENCES

1. Li Z, Conti PS. Radiopharmaceutical chemistry for positron emission tomography. *Adv Drug Deliv Rev.* 2010;62:1031–1051.
2. Wester HJ, Hamacher K, Stocklin G. A comparative study of N.C.A. fluorine-18 labeling of proteins via acylation and photochemical conjugation. *Nucl Med Biol.* 1996;23:365–372.
3. Vaidyanathan G, Zalutsky MR. Synthesis of N-succinimidyl 4-[^{18}F]fluorobenzoate, an agent for labeling proteins and peptides with ^{18}F. *Nat Protoc.* 2006;1:1655–1661.
4. Kuchar M, Pretze M, Kniess T, et al. Site-selective radiolabeling of peptides by ^{18}F-fluorobenzoylation with [^{18}F]SFB in solution and on solid phase: a comparative study. *Amino Acids.* 2012;43:1431–1443.
5. Block D, Coenen HH, Stöcklin G. N.C.A. ^{18}F-fluoroacylation via fluorocarboxylic acid esters. *J Labelled Comp Radiopharm.* 1988;25:185–200.
6. Lang L, Eckelman WC. Labeling proteins at high specific activity using N-succinimidyl 4-[^{18}F](fluoromethyl) benzoate. *Appl Radiat Isot.* 1997;48:169–173.
7. Aloj L, Lang L, Jagoda E, et al. Evaluation of human transferrin radiolabeled with N-succinimidyl 4-[fluorine-18](fluoromethyl) benzoate. *J Nucl Med.* 1996;37:1408–1412.
8. Kilbourn MR, Dence CS, Welch MJ, et al. Fluorine-18 labeling of proteins. *J Nucl Med.* 1987;28:462–470.
9. Shiue CY, Wolf AP, Hainfeld JF. Synthesis of ^{18}F-labelled N-(p-[^{18}F]fluorophenyl)maleimide and its derivatives for labelling monoclonal antibody with ^{18}F. *J Labelled Comp Radiopharm.* 1989;26:287–289.
10. Toyokuni T, Walsh JC, Dominguez A, et al. Synthesis of a new heterobifunctional linker, N-[4-(aminooxy)butyl]maleimide, for facile access to a thiol-reactive ^{18}F-labeling agent. *Bioconjug Chem.* 2003;14:1253–1259.
11. Hansen CL, Kuhnast B, Hinnen F, et al. Comparison of [^{18}F]FBA and [^{18}F]FPyMe as peptide radiolabeling agents of PEPHC1 for PET imaging of EGFRvIII. *Adv Exp Med Biol.* 2009;611:405–406.
12. Cai W, Zhang X, Wu Y, et al. A thiol-reactive ^{18}F-labeling agent, N-[2-(4-^{18}F-fluorobenzamido)ethyl]maleimide, and synthesis of RGD peptide-based tracer for PET imaging of $a_v\beta_3$ integrin expression. *J Nucl Med.* 2006;47:1172–1180.
13. Lin D, Saleh S, Liebler DC. Reversibility of covalent electrophile-protein adducts and chemical toxicity. *Chem Res Toxicol.* 2008;21:2361–2369.
14. Alley SC, Benjamin DR, Jeffrey SC, et al. Contribution of linker stability to the activities of anticancer immunoconjugates. *Bioconjug Chem.* 2008;19:759–765.
15. Morales-Sanfrutos J, Lopez-Jaramillo J, Ortega-Munoz M, et al. Vinyl sulfone: a versatile function for simple bioconjugation and immobilization. *Org Biomol Chem.* 2010;8:667–675.
16. Toda N, Asano S, Barbas CF 3rd. Rapid, stable, chemoselective labeling of thiols with Julia-Kocienski-like reagents: a serum-stable alternative to maleimide-based protein conjugation. *Angew Chem Int Ed Engl.* 2013;52:12592–12596.
17. Lewis MR, Shively JE. Maleimidocysteineamido-DOTA derivatives: new reagents for radiometal chelate conjugation to antibody sulfhydryl groups undergo pH-dependent cleavage reactions. *Bioconjug Chem.* 1998;9:72–86.
18. Shen BQ, Xu K, Liu L, et al. Conjugation site modulates the in vivo stability and therapeutic activity of antibody-drug conjugates. *Nat Biotechnol.* 2012;30:184–189.
19. Baldwin AD, Kiick KL. Tunable degradation of maleimide-thiol adducts in reducing environments. *Bioconjug Chem.* 2011;22:1946–1953.
20. Vincent JP, Mazella J, Kitabgi P. Neurotensin and neurotensin receptors. *Trends Pharmacol Sci.* 1999;20:302–309.
21. Myers RM, Shearman JW, Kitching MO, et al. Cancer, chemistry, and the cell: molecules that interact with the neurotensin receptors. *ACS Chem Biol.* 2009;4:503–525.
22. García-Garayoa E, Allemann-Tannahill L, Blauenstein P, et al. In vitro and in vivo evaluation of new radiolabeled neurotensin(8-13) analogues with high affinity for NT1 receptors. *Nucl Med Biol.* 2001;28:75–84.
23. Moody TW, Chan D, Fahrenkrug J, et al. Neuropeptides as autocrine growth factors in cancer cells. *Curr Pharm Des.* 2003;9:495–509.
24. Dupouy S, Mourra N, Doan VK, et al. The potential use of the neurotensin high affinity receptor 1 as a biomarker for cancer progression and as a component of personalized medicine in selective cancers. *Biochimie.* 2011;93:1369–1378.
25. Reubi JC, Waser B, Friess H, et al. Neurotensin receptors: a new marker for human ductal pancreatic adenocarcinoma. *Gut.* 1998;42:546–550.

26. Souazé F, Dupouy S, Viardot-Foucault V, et al. Expression of neurotensin and NT1 receptor in human breast cancer: a potential role in tumor progression. *Cancer Res.* 2006;66:6243–6249.
27. Shimizu S, Tsukada J, Sugimoto T, et al. Identification of a novel therapeutic target for head and neck squamous cell carcinomas: a role for the neurotensin-neurotensin receptor 1 oncogenic signaling pathway. *Int J Cancer.* 2008;123: 1816–1823.
28. Sehgal I, Powers S, Huntley B, et al. Neurotensin is an autocrine trophic factor stimulated by androgen withdrawal in human prostate cancer. *Proc Natl Acad Sci USA.* 1994;91:4673–4677.
29. Alifano M, Souaze F, Dupouy S, et al. Neurotensin receptor 1 determines the outcome of non-small cell lung cancer. *Clin Cancer Res.* 2010;16:4401–4410.
30. Bergmann R, Scheunemann M, Heichert C, et al. Biodistribution and catabolism of ^{18}F-labeled neurotensin(8-13) analogs. *Nucl Med Biol.* 2002;29: 61–72.
31. Teodoro R, Faintuch BL, Nunez EG, et al. Neurotensin(8-13) analogue: radiolabeling and biological evaluation using different chelators. *Nucl Med Biol.* 2011;38:113–120.
32. Buchegger F, Bonvin F, Kosinski M, et al. Radiolabeled neurotensin analog, ^{99m}Tc-NT-XI, evaluated in ductal pancreatic adenocarcinoma patients. *J Nucl Med.* 2003;44:1649–1654.
33. Zhang K, An R, Gao Z, et al. Radionuclide imaging of small-cell lung cancer (SCLC) using ^{99m}Tc-labeled neurotensin peptide 8-13. *Nucl Med Biol.* 2006;33:505–512.
34. García-Garayoa E, Blauenstein P, Blanc A, et al. A stable neurotensin-based radiopharmaceutical for targeted imaging and therapy of neurotensin receptor-positive tumours. *Eur J Nucl Med Mol Imaging.* 2009;36:37–47.
35. de Visser M, Janssen PJ, Srinivasan A, et al. Stabilised ^{111}In-labelled DTPA- and DOTA-conjugated neurotensin analogues for imaging and therapy of exocrine pancreatic cancer. *Eur J Nucl Med Mol Imaging.* 2003;30:1134–1139.
36. Wu Z, Todorov I, Li L, et al. In vivo imaging of transplanted islets with ^{64}Cu-DO3A-VS-Cys^{40}-exendin-4 by targeting GLP-1 receptor. *Bioconjug Chem.* 2011;22:1587–1594.
37. Wu Z, Liu S, Hassink M, et al. Development and evaluation of ^{18}F-TTCO-Cys^{40}-exendin-4: a PET probe for imaging transplanted islets. *J Nucl Med.* 2013;54:244–251.
38. Li Z, Chansaenpak K, Liu S, et al. Harvesting ^{18}F-fluoride ions in water via direct ^{18}F-^{19}F isotopic exchange: radiofluorination of zwitterionic aryltrifluoroborates and *in vivo* stability studies. *MedChemComm.* 2012;3:1305–1308.
39. Aronin N, Carraway RE, Ferris CF, et al. The stability and metabolism of intravenously administered neurotensin in the rat. *Peptides.* 1982;3:637–642.
40. Lee YC, Uttenthal LO, Smith HA, et al. In vitro degradation of neurotensin in human plasma. *Peptides.* 1986;7:383–387.